Neurotoxicity Research (2023) 41:256–269
https://doi.org/10.1007/s12640-023-00638-3

RESEARCH ARTICLE

Pharmacological Inhibition of p-21 Activated Kinase (PAK) Restores Impaired Neurite Outgrowth and Remodeling in a Cellular Model of Down Syndrome

Natalia Barraza-Núñez[1] · Ramón Pérez-Núñez[1] · Belén Gaete-Ramírez[1] · Alejandra Barrios-Garrido[1] · Christian Arriagada[3] · Karen Poksay[4] · Varghese John[5] · Jean-Vianney Barnier[6] · Ana María Cárdenas[7] · Pablo Caviedes[1,2]

Received: 11 September 2022 / Revised: 27 December 2022 / Accepted: 10 February 2023 / Published online: 3 March 2023

Abstract

Down syndrome (DS) is characterized by the trisomy of chromosome 21 and by cognitive deficits that have been related to neuronal morphological alterations in humans, as well as in animal models. The gene encoding for amyloid precursor protein (APP) is present in autosome 21, and its overexpression in DS has been linked to neuronal dysfunction, cognitive deficit, and Alzheimer's disease-like dementia. In particular, the neuronal ability to extend processes and branching is affected. Current evidence suggests that APP could also regulate neurite growth through its role in the actin cytoskeleton, in part by influencing p21-activated kinase (PAK) activity. The latter effect is carried out by an increased abundance of the caspase cleavage-released carboxy-terminal C31 fragment. In this work, using a neuronal cell line named CTb, which derived from the cerebral cortex of a trisomy 16 mouse, an animal model of human DS, we observed an overexpression of APP, elevated caspase activity, augmented cleavage of the C-terminal fragment of APP, and increased PAK1 phosphorylation. Morphometric analyses showed that inhibition of PAK1 activity with FRAX486 increased the average length of the neurites, the number of crossings per Sholl ring, the formation of new processes, and stimulated the loss of processes. Considering our results, we propose that PAK hyperphosphorylation impairs neurite outgrowth and remodeling in the cellular model of DS, and therefore we suggest that PAK1 may be a potential pharmacological target.

Keywords P21-activated kinase · Amyloid · Down syndrome · Trisomy · Cytoskeleton · Neurites

Introduction

Down syndrome (DS) is the chromosomal aneuploidy that most frequently survives gestation (Hassold and Hunt 2001), and it represents one of the most frequent genetic disorders, with a prevalence of 14.4/10,000 live births in the USA in the period 2010 to 2014 (Mai et al. 2019) and 10.1/10,000 live births between 2011 and 2015 in Europe (Graaf et al. 2020). DS is caused by the total or partial trisomy of chromosome 21 (Antonarakis et al. 1993), which was fully sequenced by Hattori et al. (2000). Among the physical alterations in DS patients, we can find an increased incidence of congenital heart defects (Cullum and Liebman 1969) and acute leukemia in childhood (Krivit and Good 1957; Fong and Brodeur 1987), immune system and endocrine alterations, greater risk of reduced bone mineral density, and type 1 diabetes (Whooten et al. 2018). However, intellectual disability in DS patients is the most striking

✉ Pablo Caviedes
pcaviedes@ing.uchile.cl

1 Program of Molecular & Clinical Pharmacology, ICBM, Faculty of Medicine, University of Chile, Santiago, Chile

2 Center for Biotechnology & Bioengineering (CeBiB), Department of Chemical Engineering, Biotechnology & Materials, Faculty of Physical & Mathematical Sciences, University of Chile, Santiago, Chile

3 Department of Anatomy & Forensic Medicine, Faculty of Medicine, University of Chile, Santiago, Chile

4 Ultragenyx Pharmaceuticals, Novato, CA, USA

5 Department of Neurology, Easton Center for Alzheimer's Disease Research, University of California, Los Angeles, CA, USA

6 Neuroscience Paris-Saclay Institute, UMR 9197, CNRS-Université Paris-Saclay, Gif-Sur-Yvette, France

7 CINV, University of Valparaíso, Valparaíso, Chile

feature. In addition, these patients undergo early development of Alzheimer's disease (AD) neuropathology and dementia (Strydom et al. 2018). From the neuropathological point of view, morphological alterations are evident in DS patients, including smaller brain size and occipitofrontal circumferences, as well as delayed myelination in fibers of the frontotemporal lobe (Wisniewski et al. 1990). Moreover, altered dendritic morphology in pyramidal neurons from the cerebral cortex of DS-old infants (over 4 months old) has also been documented, namely short basilar dendrites, decreased number of dendritic spines, and an unusual length of thin spines (Takashima et al. 1981). Morphological alterations have also been observed in animal models of DS, as has been described in the cerebral cortex of the Ts65Dn mouse model, where it has been found that pyramidal cells have smaller dendrites, with less arborization and fewer dendritic spines compared to control mice (Dierssen et al. 2003). Other studies have further shown that the axon length and the number of branches were decreased in hippocampal neurons of Ts65Dn mice in the early postnatal period (Jain et al. 2020). Similar results were described in human models such as in patient iPSC-derived neurons (Huo et al. 2018). Taken together, these data provide evidence that the neuronal architecture is compromised in DS. At present, it is estimated that the excess gene dosage derived from the trisomic condition directly or indirectly underlies the deleterious effects of DS (Pritchard and Kola 1999).

Clearly, the most striking and limiting feature for persons with DS is intellectual disability. Although efforts have been made to search for therapeutic targets to address this dysfunction, these have been insufficient. Indeed, as seen in the ClinicalTrials.gov webpage, only around 50 trials are currently active in Down syndrome, and only a handful address cognitive impairment. More recent studies addressing DS-related intellectual disability include pulsatile treatment with GnRH, which reportedly improves cognition in patients with DS (Manfredi-Lozano et al. 2022), and treatment with green tea extracts containing epigallocatechin-3-gallate (EGCG), an inhibitor of Dyrk1a, in a trisomic DS mouse model (Ts65Dn) (De Toma et al. 2019; De Toma et al. 2020). Although these studies have not currently been successful, they point to the option of targeting cell signaling pathways that can be related to cognitive function.

Among the genes found in chromosome 21 that are overexpressed in DS (Korenberg et al. 1989), which are also related to dementia and Alzheimer's-like neuropathology, is that of the Amyloid Precursor Protein (APP). APP is an integral membrane protein that comprises a trans-membrane domain, a large N-terminal ectoplasmic region, and a short cytoplasmic C-terminal domain. The transmembrane domain includes part of the Aβ peptide sequence. The C-terminal of APP is cleaved by caspase at the aspartate residue 664 (ASP664), generating a 31 amino acid fragment (C31), which has also been related to neurotoxicity (Lu et al. 2000; Weidemann et al. 1999).

Apart from its role in neuronal development through extracellular matrix interaction, APP may also play an important role in neurite outgrowth, by regulating actin cytoskeleton dynamics through the p21-activated kinases (PAKs) pathway. In this regard, a study by McPhie et al. (2003) demonstrated the interaction of the C-terminal domain of APP with PAK3 in a region adjacent to the CDC42 and Rac1 binding sites of PAK3.

Furthermore, the platelet-derived growth factor, b-chain promoter APP (PDAPP) transgenic mouse, an animal model of AD, exhibits changes in PAK phosphorylation when caspase cleavage is inhibited at the aspartate 664 residue from the APP C-terminus (Nguyen et al. 2008). PAKs play a central role in cell signaling and are the main kinase effectors of Rho GTPases belonging to Rac1 and Cdc42 family (Bokoch 2003; Kreis and Barnier 2009; Manser et al. 1994; Martin et al. 1995). After being activated by Rac and Cdc42, PAKs interact directly with LIMK, which in turn phosphorylates cofilin. The latter, when phosphorylated, inhibits actin depolymerization (Edwards et al. 1999; Pérez-Núñez et al. 2016). PAKs are fundamental in cytoskeleton dynamics during processes such as cell movement, filopodia formation and dissolution of focal complexes, actin stress fibers, and focal adhesions (Manser et al. 1997; Zhou-Shen et al. 1998; Bokoch 2003). Furthermore, mutations in the brain-specific PAK isoform PAK3 have been found to underlie non-syndromic mental retardation linked to chromosome X, thus positioning the PAK pathway as a relevant mechanism in the neuronal connectivity and hence cognitive function (Allen et al. 1998; Rousseau et al. 2003). In addition, PAK3 has been associated with an important role in the formation of dendritic spines, as well as in the regulation of mechanisms related to the reorganization of synaptic networks (Kreis et al. 2007; Dubos et al. 2012).

Then, the interaction between APP and/or its derived peptides might trigger PAKs overactivation, promoting alterations in downstream effectors of PAK such as LIMK and cofilin, modifying cell cytoskeleton through actin dynamics, and thus leading to impairments in neuronal development such as those encountered in AD and DS pathologies.

Considering the alterations observed at the morphologic level in DS human brains and animal models, it would be interesting to study whether inhibition of PAK overactivation restores neurite outgrowth in a cell model of DS where APP is reportedly overexpressed (Rojas et al. 2008). This cell model, named CTb, was established from the cerebral cortex of a mouse with trisomy 16, whereas a control line, named CNh, was developed from the cerebral cortex of a normal, euploid littermate (Cárdenas et al. 1999). As PAK1 is the most abundantly expressed isoform in CTb and CNh cells (Pérez-Núñez et al. 2016), we focused on evaluating its

phosphorylation and the effects of its inhibition on neurite dynamics. Therefore, in the present work, we evaluated how the inhibition of PAK1 activity with the specific inhibitor FRAX 486 influences neurite growth in the trisomic cell line CTb. We quantified the number and length of neurite processes by Sholl analysis and further established six algorithms to quantify neurite dynamics. Our studies suggest that the pharmacological inhibition of PAK hyperphosphorylation in CTb improves the branching of cell processes.

Materials and Methods

Cell Line Cultures

CTb and CNh cells were maintained in DMEM/F12 (GIBCO, NYSE-TMO) supplemented with 15 mM HEPES, 1 g/l bicarbonate, 40 mg/l gentamicin, and 5 mg/l ketoconazole, 10% (v/v) adult bovine serum, and 2.5% fetal bovine serum, at 37 °C, 100% humidity, and 5% atmospheric CO2. For cell passages, cells were detached with 0.2% trypsin (Invitrogen, Grand Island, NY) for 5 min at 37 °C.

Cell Differentiation

Cell differentiation was performed by incubating CTb cells for 72 h with Neurobasal/B27 medium (Gibco, NYSE-TMO), ketoconazol 5 mg/L, 100 ng/ml basic fibroblast growth factor (bFGF) (ProSpec-Tany, Ness-Ziona, Israel), and 10 µM forskolin (FK) (cat. Ab120058, Abcam, Cambridge, MA, USA), as previously described (Pérez-Núñez et al. 2016).

Western Blot

Protein lysis was performed with RIPA (radioimmunoprecipitation assay) buffer (150 mM NaCl, 1% NP-40, 0.5% sodium deoxycholate, 0.1% SDS, and 50 mM Tris, pH 8.0) and protease inhibitor tablets (Complete, ultra, mini, EDTA-free, easy pack, Roche®) and phosphatases (PhosSTOP Roche, Mannheim, Germany). Sonication was performed for 30 s, and centrifugation at 14,000 rpm for 15 min at 4 °C. Quantification was performed with a Coomassie reagent/Bradford protein assay kit (Thermo Scientific™, Rockford, IL, USA). Then, the protein extract was mixed with loading buffer 5×(10% SDS, 50% glycerol, 12.5% 2-mercaptoethanol, 0.0010% bromophenol blue, and 312.5 mM Tris 1 M pH 6.8), electrophoretically separated on a 10% polyacrylamide gel, and transferred to a polyvinylidene difluoride membrane for 1.5 h at 400 mA. Membrane blocking was performed with 5% bovine serum albumin (BSA) in phosphate-buffered saline in (PBS; 137 mM NaCl, 2.68 mM KCl, 10 mM Na_2HPO_4, 1.76 mM KH_2PO_4) containing 0.1% Tween-20, and membrane washes were performed with PBS with 0,1% Tween-20.

Membranes were incubated in MAB 348, anti-APP A4 monoclonal antibody against residues 66–81 of APP (N-terminus), clone 22C11 (Merck Millipore, Darmstadt, Germany) for detection and quantification of total APP. An anti-beta tubulin antibody (TUB 2.1), ab11308 (Abcam) was used for loading control. Caspase cleavage of the C-terminus of APP was assessed with the APPΔC31 antibody, pAB ENZ-ABS445, (Enzo Life Sciences, Inc., donated by the Bredesen lab, Buck Institute, Novato, CA, USA). Phosphorylated PAK1 was determined with the anti-PAK1 (phospho S204) antibody ab79503 (Abcam). For the detection of total PAK1, anti-PAK1 antibody ab40852 (Abcam) and for secondary antibody anti-rabbit (HRP) ab6802 (Abcam) were used. The proteins were detected using the chemiluminescence kit Super Signal West Pico Chemiluminescent Substrate (Thermo Scientific, Rockford, IL, USA). Densitometric analyses were performed with the Image J program (NIH, Bethesda, USA).

Treatment with FRAX 486

An MTT (3-[4,5-dimethylthiazol-2-yl]-2,5 diphenyl tetrazolium bromide) assay was performed to determine the lethal dose 50 (LD50) of FRAX 486 (cat. A13691, AdooQ Bioscience, Irvine, CA, USA). A curve was constructed with the following concentrations in nM: 50, 500, 1000, 5000, 7000, and 10,000. The viability percentage was determined relative to control cells using the following formula:

$$\%\text{Viability} = \frac{\text{OD of treated cells}}{\text{OD of control cells}} \times 100$$

Then, the concentration versus percentage survival curve was constructed, and the LD50 was calculated.

Measurement of Caspase Activation

The quantification of the activity of total caspases in the cell lines was carried out with the FAM (carboxyfluorescein)-FLICA (Fluorescent Labeled Inhibitors of Caspases) in vitro Caspase Detection Kit (Immunochemistry Technologies, Davis, CA, USA), according to the manufacturer's instructions. CNh and CTb cells were seeded in 60-mm dishes, and the following day the recommended volume of FLICA (300 µl for 5×10^5 cells/ml) was added to each condition. Samples were evaluated on a FACSort cytometer (Becton Dickinson) and analyzed using FlowJo™ v10.4 software (BD Life Sciences). The analyses were performed with at least 10,000 events from the total population for each condition, and the percentage of cells labeled with FLICA within this population was determined.

Sholl Analysis

To analyze neurite processes in cultured cells, Sholl analyses were performed as described by Pérez-Núñez et al. (2016) and were carried out in the cell lines after 72 h of differentiation. Image acquisition was made with an INFINITY X-32C camera (Lumenera Corporation, Ottawa, Ontario, Canada), using a Lieder phase-contrast microscope (Model: MI-535), with a 10X objective. Pseudoimages were first created with the public domain Image J software (NIH, Bethesda, USA) to perform the neurite arborization study, and we used the Neuron J program (Image J plugin, NIH, Bethesda, USA) for length analysis. Cell arborization was analyzed with a superimposed template of concentric rings. The first ring was set at a distance equivalent to twice the radius of the soma of each cell analyzed, and the following rings were placed 5 µm apart from each other. The number of crossings of each process and each intersection of a ring with a neurite was quantified. Neurite length analysis was performed with the public domain NeuronJ program, in which the length of each process was measured and then the average length of neurites was quantified for each cell analyzed.

Neurite Outgrowth Analysis

We evaluated a branching pattern called the *branching index (BI)*, as described by García-Segura and Pérez-Márquez (2014). The BI quantifies new processes formed from one ring to another in Sholl analysis. In other words, it subtracts the number of crossings in the inner ring (closer to the soma) from the number of crossings observed in the outer ring (further from the soma). If the difference between these two rings (the inner ring and the outer ring) returns a positive value, it means that the number of crossings from one ring to another increase, and if the difference between the two rings gives a negative value, it means that the number of crossings between one ring and another decreases. To quantify new processes that formed from one ring to another, negative values were converted to zero, and the positive values were multiplied by the respective radius in which they were encountered. The algorithm that defines BI is shown in Table 1. A high value of BI in any given cell may be due to either a greater number of processes and/or a greater distance of the said processes from the soma.

Table 1 Morphologic parameters evaluated in Sholl analysis cell lines

Algorithms used to evaluate the growth of cellular processes.	
$BI=\sum(\text{intersections circle}_n - \text{intersections circle}_{n-1})r_n$	Subtracting the number of crossovers that were observed in the outer ring (further from the soma) minus the number of crossovers in the inner ring (closer to the soma) and the positive values were multiplied by the respective radius in which they were found (*García-Segura and Pérez-Márquez 2014*).
$RBI_{cellular} = \frac{d(p)}{\text{distance between rings}}$ **d** = distance from the farthest soma at which new processes were created. **p** = position of the farthest ring where the cell created processes.	Only takes into account the positive value that was obtained farthest from the soma for each cell analyzed, this value is transformed into a value of one and then multiplied by the radius at which it is located and divided by the distance between the sholl rings, which in this case is five.
$OBI_{cellular} = \sum_{i=1}^{12} c(i)$ **c(*i*)** = number of new observable processes in ring i.	Sum of all the positive values obtained from the initial subtraction between rings.
$DBI= \sum (\text{intersections circle}_n - \text{intersections circle}_{n-1})r_n$	The positive values of initial subtracting are the ones that become zero and the negative values are kept, then transformed to a positive value and multiplied by the ring in which the process loss was made.
$RDBI_{cellular} = \frac{d(p)}{\text{distance between rings}}$ **d** = distance from the farthest soma where processes were lost. **p** = position of the farthest ring where the cell lost processes.	Only takes into account the negative value that was obtained farthest from the soma for each cell analyzed, this value is transformed into a positive value of one and then multiplied by the radius at which it is located and divided by the distance between the sholl rings, which in this case is five.
$ODBI_{cellular} = \sum_{i=1}^{12} c(i)$ **c(*i*)** = number of processes that were lost in ring i.	All the negative values obtained in the initial subtraction between rings, were transformed into a positive values and then added.

In this work, we design five new indexes, which were obtained by modifying the BI index. Thus, we modified the BI index to yield the *radial branching index (RBI)*, which quantifies the cell branching capacity away from the soma independently of the number of new processes created. In this way, a higher RBI value would indicate a greater capacity of the cell to create new processes far from the soma; moreover, those cells that coincide in that the creation of new processes was in the same ring farther from the soma will have the same RBI value, as can be seen in Table 1.

In contrast to RBI, we used the index called the *observed branching index (OBI)* (Table 1) to quantify the ability to create new processes independent of the distance from the soma; therefore, all newly formed processes are added independently of their distance from the soma; thus, a higher value of OBI indicates more processes created.

The aforementioned algorithms can help us to identify the new processes that are formed from one ring to another in Sholl analysis. However, approximately 60% of the process formation data corresponds to zero (BI-RBI-OBI). On the other hand, approximately 90% of the analyzed cells obtained negative values when calculating the difference in crossings between the outer ring and the inner ring. Negative values indicate that there was a decrease or loss of processes between one ring and another; that is, it can provide us with valuable information on how the cell branched, regardless of the new processes that were formed along the way. Therefore, we observe that the loss of processes as it moves away from the soma increases, and we can measure it with the *decreased branching index (DBI)* algorithm (Table 1). In order to know the farthest distance from the soma in which processes are lost, we modified the RBI algorithm by *radial decrease branching index (RDBI)* (Table 1), which quantifies the farthest distance (from the cell soma) in which processes are lost. To know the total number of processes that are lost for each analyzed cell, we modified the OBI algorithm by the *observed decreased branching index (ODBI)* (Table 1). This algorithm allows us to indirectly know the cellular branching, independent of the new processes that were formed. All these analyzes were performed with the Python program version 3.6.13 and IDE Spyder version 5.0.5.

Statistical Analysis

All statistical analyses were performed with GraphPad Prism version 9.4.1 for macOS (GraphPad Software, www.graphpad.com, San Diego, California, USA). Statistical significance between datasets was determined by the Mann–Whitney test and unpaired t-test for p levels < 0.05.

Results

PAK Phosphorylation Is Increased in CTb Cells

Due to the syntheny between mouse autosome 16 and human chromosome 21, murine trisomy 16 (Ts16) is an animal model of DS (Oster-Granite 1986). However, due to the inviability of the model, we used CTb cells, a cellular immortalized cell model of DS that were established from the cerebral cortex of a mouse with trisomy 16, and a control line CNh extracted from the cerebral cortex of a normal euploid littermate.

The signaling pathway related to the interaction between APP and PAK isoform in a region adjacent to the Rac1/CDC42 binding domain between amino acid residues 93 and 126 of PAK3 (McPhie et al. 2003) called our attention. Therefore, we first determined whether the trisomic cell line CTb displays the conditions that might favor PAK1 hyperphosphorylation, and therefore, we measured the expression of APP. As we previously reported (Rojas et al. 2008; Opazo et al. 2006), APP is overexpressed in the CTb cell line compared to CNh cells (Fig. 1a). As C-terminal cleavage of APP is produced by the action of caspases, we then evaluated the state of activation of total caspases with the FLICA marker. As shown in Fig. 1b, a greater activation of total caspases is evident in the trisomic cell line CTb, when compared to CNh cells. Next, to determine whether the caspase-mediated cleavage at the C-terminal end of APP to yield the C31 peptide is indeed present, we used an antibody that can label the APPΔC31 fragment. This antibody binds to the epitope that remains after the peptide is cleaved at the C-terminus of APP. In Fig. 1c, a higher proportion of APPΔC31 can be observed in the CTb cells when compared to its control CNh cells. Finally, we compared PAK1 phosphorylation in both cell lines. As shown in Fig. 1d, phosphorylated PAK1 (p-PAK1) is found in a greater proportion in the trisomic CTb cell line when compared with its control cell line CNh.

Inhibition of PAK1 Phosphorylation Improves Neuronal Morphology in CTb Cells

To assess the impact of PAK phosphorylation on cell morphology, CTb cells were incubated with Neurobasal-B27 medium with FK and bFGF for 72 h. This treatment that promotes cell differentiation and neurite outgrowth (Pérez-Núñez et al. 2016) was carried out in the absence or the presence of the specific PAK inhibitor, FRAX 486.

We first determined the LD50 of FRAX 486 in CTb cells using different concentrations of this inhibitor. The LD50 for FRAX 486 was found to be 6.4 µM. Therefore, considering

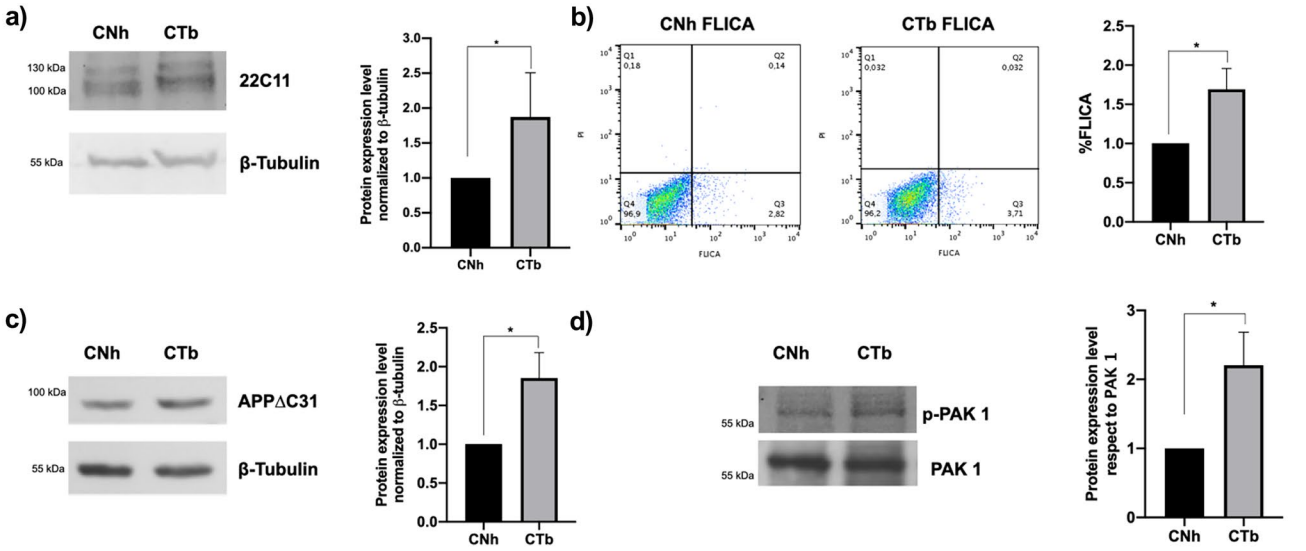

Fig. 1 Expression of p-PAK and factors associated with its activation in CNh and CTb cells. **a** A representative western blot and quantification of APP protein levels, as evaluated with the 22C11 antibody, normalized to β-tubulin in CNh and CTb cell lines in basal conditions, without differentiation ($n=4$). **b** Evaluation of caspase activation with FLICA assay ($n=4$). **c** A representative western blot of the APPΔC31 fraction and its quantification ($n=7$). **d** Representative western blot of phosphorylated PAK1 (p-PAK1) expression in CNh and CTb cell lines in basal conditions, without differentiation and its quantification normalized to PAK1 ($n=4$). Bars represent the mean with SEM. * $p<0.05$ (Mann–Whitney test)

the previous antecedents, the concentration of FRAX 486 that we used in our work was 50 nM (Harms et al. 2018; Licciulli et al. 2013).

Process length and complexity were quantified by Sholl analysis. Figure 2a shows a representative cell in culture and the respective pseudoimage. Figure 2b presents the respective Sholl and the process length analysis. The chemical structure of the PAK inhibitor, FRAX486 (Dolan et al. 2013), is displayed in Fig. 2c. The result of the process length analysis shows a significant increment of neurite length in CTb cells after treatment with FRAX 486 (Fig. 2d). Additionally, Sholl analysis in CTb cells indicates that FRAX 486 increases complexity in short neurites (< or = 20 µm), since the number of crossings in the Sholl rings increased significantly in the rings close to the soma (0, 10, 15, and 20 µm from the soma) after treatment with FRAX 486 (Fig. 2e).

New Algorithm for Neurite Outgrowth Analysis: FRAX 486 Favors the Formation of New Processes and Stimulates a Greater Loss of Processes

Although new variants of the Sholl analysis have been described in a more automated way (Binley et al. 2014) and for certain neuronal types (López-Cabrera et al. 2020), we developed six algorithms (based on the branching index described by García-Segura and Pérez-Márquez (2014) that quantify the gain or loss of processes as that processes move away from the soma.

If we consider that FRAX 486 treated CTb cells exhibited an increased number of crossings in the first rings in our Sholl analysis, we speculated that the presence of this inhibitor could increase the process branching in the trisomic cell line CTb. Therefore, to assess cell branching and answer these questions, we formulated a series of algorithms that can quantify both formation of new processes (BI-RBI-OBI) and the loss of processes (DBI-RDBI-ODBI) from one ring to another in our Sholl analysis (Table 1).

Some examples of the morphological evaluation on the cell line CTb can be seen in Fig. 3, which shows different representative images of these cells with Sholl analysis, and in the box on the right, their respective rates of formation and loss of processes. In such a fashion, the values can be compared with respect to the range and average of the indexes in the entire cell culture (these values are presented in the two columns in the center of the table). Figure 3a shows two primary processes without the formation of secondary processes, which is reflected by a BI index = 0. The images in Fig. 3b show a cell that forms a new process (OBI: 1) of 25 µm from the soma (RBI: 5). In Fig. 3c, an above-average BI index is observed (BI: 170, mean of BI: 14), which depicts a cell that formed six new processes (OBI: 6), and the one that was created farthest was 50 µm from the soma (RBI:10). A similar pattern is observed with the process loss indices, where the DBI value increased in relation

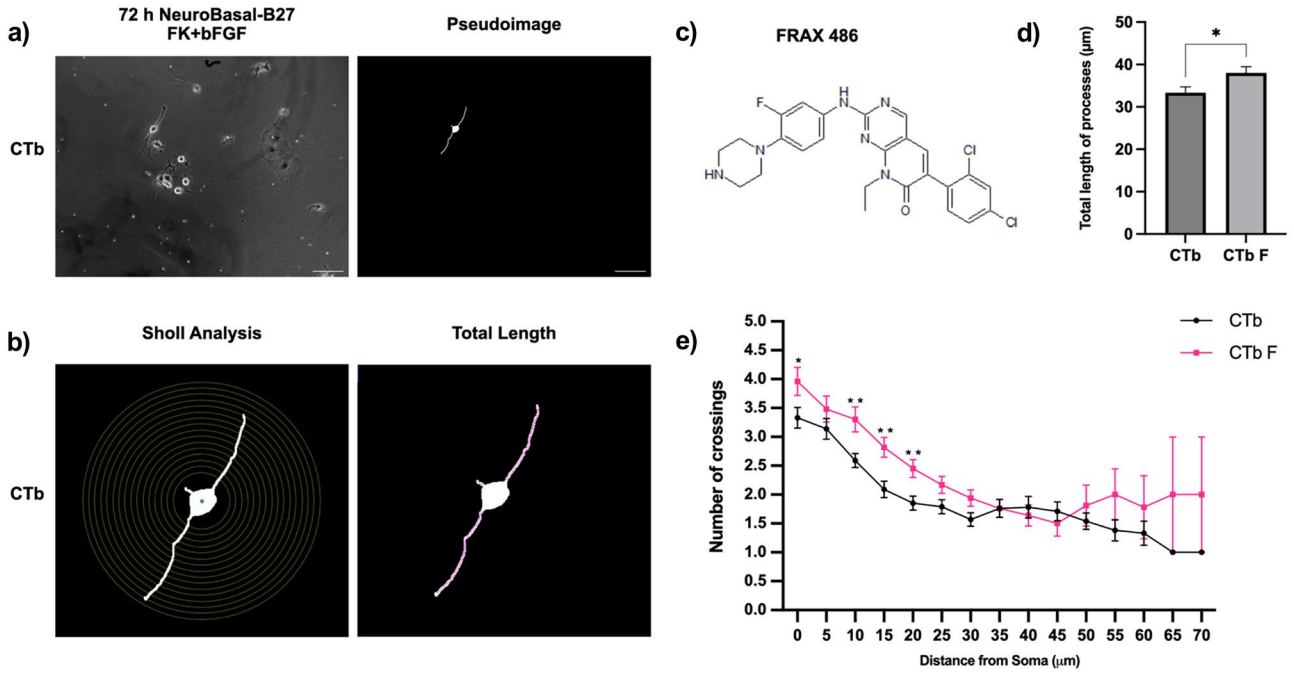

Fig. 2 Sholl and length analysis of cell processes after FRAX 486 treatment in CTb cell lines. **a** Representative images of Sholl analysis in CTb cells maintained with Neurobasal-B27 medium with forskolin (FK) and bFGF during 72 h. Scale bar = 100 µm; the left panel shows a pseudoimage of the Sholl analysis. **b** Representative images of concentric rings of Sholl analysis; the left panel shows a process length analysis. **c** Molecular structure of FRAX 486. **d** Quantification of the total length of processes in CTb cells without (CTb, $n = 237$) or with FRAX 486 treatment (CTb F, $n = 314$). **e** Sholl analysis shows the number of crossings versus distance from soma with significant differences between CTb and CTb F in the ring 0, 10, 15, and 20 µm. Each point represents the mean with SEM. $^{*}p < 0.05$, $^{**}p < 0.01$ (unpaired t-test)

to average values (DBI: 275, mean of DBI: 71), due to the loss of several processes (ODBI: 8), and the one that was lost farthest was 60 µm from the soma (RDBI: 12) (Fig. 3c).

These algorithms that quantify the formation and loss of neuronal cell processes can help us study morphological patterns observed in the cells in basal conditions, without FRAX 486 treatment, and consequently identify changes that may occur in response to a stimulus. For this reason, we then evaluated the parameters of formation and process loss in the trisomic cell line, after treatment with FRAX 486. The means of the values obtained with the algorithms were plotted in Fig. 4. Branching index (BI), observed branching (OBI), and radial branching index (RBI) were represented in Fig. 4a–c, respectively, being only the OBI index significantly increased in the presence of FRAX 486. This indicates that FRAX 486 increased the amount of new processes that are formed from one ring to another. Furthermore, as shown in Fig. 4d–f, FRAX 486 also increased the decreased branching index (DBI), observed decreased branching index (ODBI), and radial decrease branching index (RDBI), suggesting that PAK inhibition induces loss of processes that are farther from the soma.

Discussion

The relationship between cognitive dysfunction in patients with DS with a neuronal morphological impairment drew our attention. Reportedly, patients with DS have less brain tissue (Pinter et al. 2001) and reduced hippocampus and cerebellum size (Raz et al. 1995). Also, patients exhibit morphological abnormalities in the dendritic spines of pyramidal neurons in the motor cortex (Marin-Padilla et al. 1976). Cognitive alterations can vary with aging, and the trisomy on chromosome 21 can favor the onset of early dementia, as highlighted in the study by McCarron et al. (2017). This study followed 77 patients with DS for 20 years and concluded that 97.4% of the subjects studied developed dementia, where the mean age of diagnosis was 55. Early dementia in patients with DS has also been related to Alzheimer-type dementia, and one of the proteins that characterize AD as the precursor of senile plaques (SP) is the APP, whose gene is present on chromosome 21. In this regard, the brains of DS patients develop SP quite early in life (Masters et al. 1985; Kang et al. 1987). Furthermore, as previously reported, a 78-year-old patient with partial trisomy of chromosome 21, where

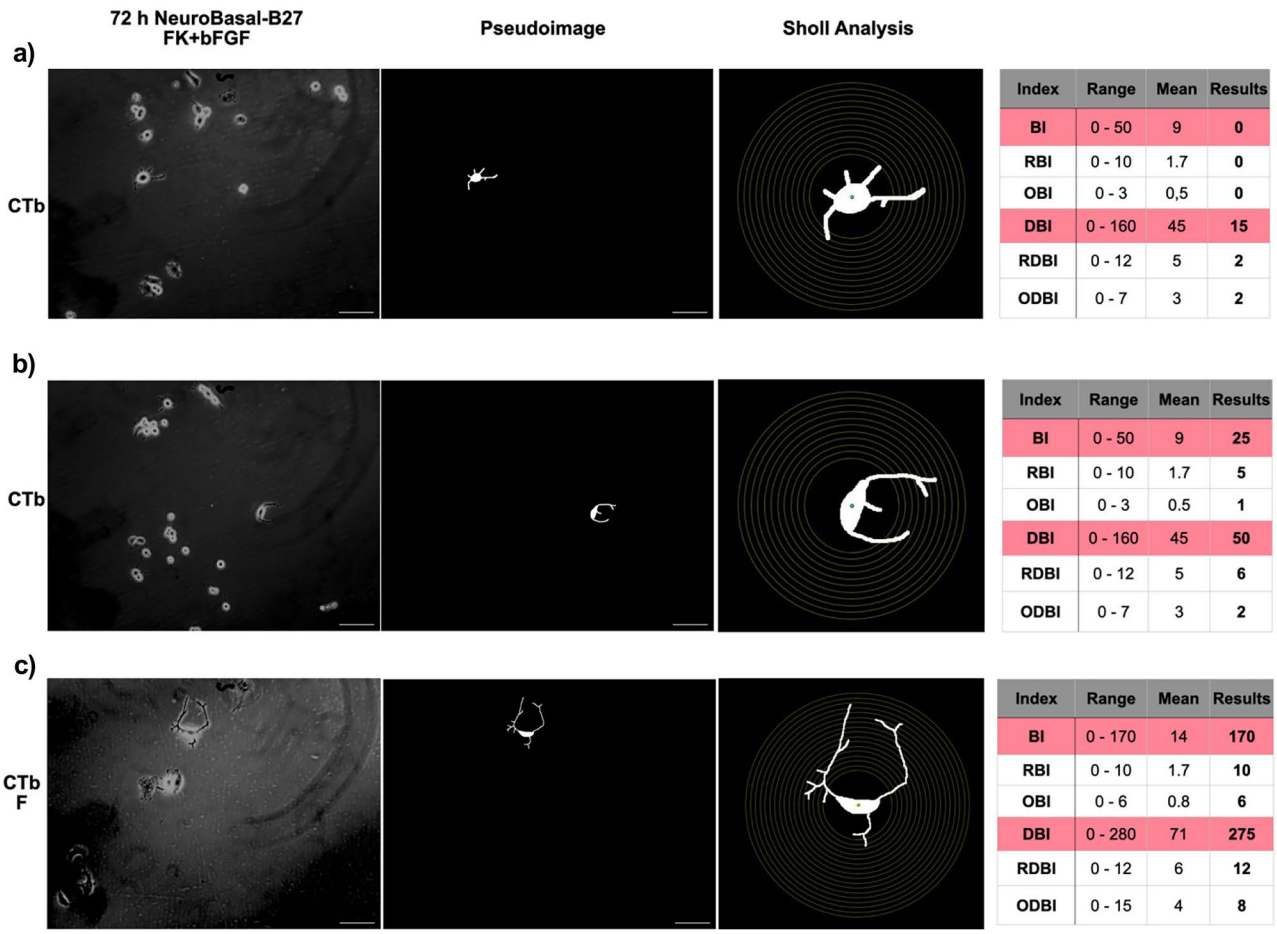

Index	Range	Mean	Results
BI	0 - 50	9	0
RBI	0 - 10	1.7	0
OBI	0 - 3	0,5	0
DBI	0 - 160	45	15
RDBI	0 - 12	5	2
ODBI	0 - 7	3	2

Index	Range	Mean	Results
BI	0 - 50	9	25
RBI	0 - 10	1.7	5
OBI	0 - 3	0.5	1
DBI	0 - 160	45	50
RDBI	0 - 12	5	6
ODBI	0 - 7	3	2

Index	Range	Mean	Results
BI	0 - 170	14	170
RBI	0 - 10	1.7	10
OBI	0 - 6	0.8	6
DBI	0 - 280	71	275
RDBI	0 - 12	6	12
ODBI	0 - 15	4	8

Fig. 3 Relationship between cell morphology and indexes of process formation and loss. This figure shows representative images of a CTb cell with different morphology. From left to right, images represent the cell under the phase-contrast microscope, the pseudoimage, its Sholl analysis, and the respective indexes of formation and loss of processes. **a** Image of CTb cell with $BI = 0$, without formation of new processes. Regarding the index of loss of processes, it indicates that the cell lost two processes (ODBI: 2), and the one that was lost the farthest was 10 µm from the soma (RDBI: 2). **b** The image shows a CTb cell with a new process formed (OBI: 1) 25 µm from the soma (RBI: 5). RDBI: 6 and ODBI: 2 indexes show that two processes were lost in this particular cell, and the one that was lost furthest was 30 µm from the soma. **c** Image of CTb F cell. The indexes indicate that the cell formed six new processes (OBI: 6), and the one that was created furthest was 50 µm from the soma (RBI: 10). The process loss index indicates that the cell lost eight processes in total (ODBI: 8), and the one that was lost furthest was 60 µm from the soma (RDBI: 12), as can be seen in the image. Scale bar = 100 µm

the APP gene was present in only two copies, did not show signs of dementia (Prasher et al. 1998). Furthermore, a case report by Doran et al. (2017), who reported the situation of an aged DS patient who had a deletion of the APP gene in one of the triplicated chromosomes and also lacked signs of dementia, in addition to low levels of Aβ peptide in plasma and an absence of Alzheimer's-like neuropathology. This information highlights the importance of APP in the development of dementia in older DS patients and its relation to neuronal alterations at a morphological level.

Structural alterations in cell morphology can also be observed in our trisomic model CTb, compared to its control, CNh cells; among them is the reduction in the number of neurites that cross each ring in Sholl analysis, shorter process length, and higher F-G actin ratio (Pérez-Núñez et al. 2016).

Due to the aforementioned, in the present study, we focused on the search for therapeutic targets that can serve as research points/focuses and which may potentially revert or mitigate the structural alterations observed in a trisomic cell model. To direct the search for therapeutic targets that have a direct impact on the cell cytoskeleton, we focused on studying the p21-activated kinase 1, PAK 1, and its influence on neurite outgrowth. Since PAK1 has been related to the formation, maturation, and stability of dendritic spines in primary cultured neurons (Hayashi et al. 2007a). Furthermore, phosphorylated PAK can also be found colocalized with F-actin in the growth cone (Rashid et al. 2001). Indeed, double knockout mice for PAK1 and PAK3 show reduced process complexity than the wild type, as well as enhanced cofilin activity and reduced amounts of F-actin (Huang et al. 2011). In addition, previous

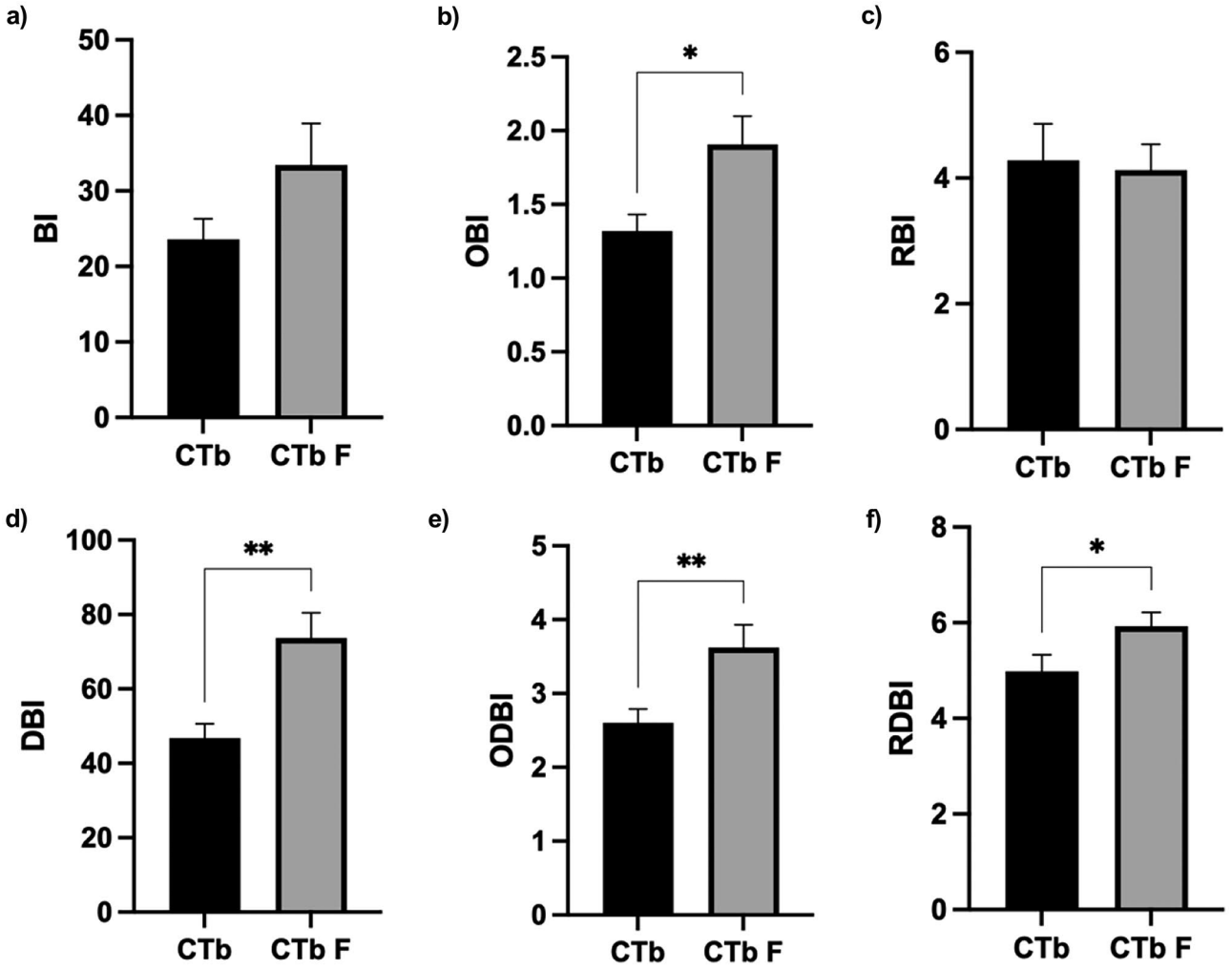

Fig. 4 Morphologic parameters in CTb after treatment of FRAX 486. **a** Branching Index (BI). **b** Observed branching Index (OBI). **c** Radial branching index (RBI). **d** Decrease branching index (DBI). **e** Observed decreased branching index (ODBI). **f** Radial decrease branching index (RDBI). Values represent the mean with SEM. *: Significant for $p < 0.05$. **: significant for $p < 0.01$ (unpaired t-test)

studies indicate that protein activation could be influenced by the cleavage in the C-terminal of APP (Nguyen et al. 2008).

In this regard, we evaluated in our trisomic line the conditions that could influence PAK activation, such as APP overexpression (Fig. 1a) and enhanced caspase–dependent cleavage in the C-terminal segment of APP (Fig. 1c) produced by the action of caspases (Fig. 1b). In agreement with these results, we observed that PAK1 is hyperphosphorylated in the trisomic cells (Fig. 1d). Accordingly, inhibition of PAK1 increased neurite length (Fig. 2d) and the number of crossings per Sholl ring (Fig. 2c) in CTb cells. Furthermore, FRAX 486 increased the number of new processes formed from one ring to another (Fig. 4b), although it does not influence the length of the new formed processes (Fig. 4c). On the other hand, FRAX 486 also stimulates the loss of neurites (Fig. 4d–f), suggesting that PAK inhibition favors neurite remodeling and branching in CTb cells.

In this regard, previous studies have shown the impact that FRAX 486 can have on increasing cell proliferation and in the rescue of neurogenesis defects in DS iPSC-derived cerebral organoids (Tang et al. 2021), thus strongly suggesting the importance of the PAK pathway in neuronal development. In agreement with this study, we can observe that abnormal activation of the PAK pathway influences structural changes in cell morphology during process growth, as described by Pérez-Nuñez et al. (2016) regarding the effect of overexpressed DSCAM in PAK. Yet, the latter effect is phasic rather than tonic. Our present study addresses a different deregulation mechanism associated to specific DS-related overexpressed genes, such as APP, which in turn may possibly have a tonic effect. Furthermore, overexpressed APP has an important role in the pathogenesis of Alzheimer's-like dementia that develops in aged DS patients (Doran et al. 2017). Hence, PAKs may

be deregulated cooperatively by at least two DS-related overexpressed genes (DSCAM, APP) in two different fashions: phasic and tonic. Taken together, PAK appears as a common downstream effector of both excess gene products and presents this kinase as an interesting target for pharmacological modulation.

We acknowledge, however, that more studies are required to confirm these findings. Yet, the results described herein suggest the following model described in Fig. 5, which relates the impact of APP and PAK on the actin cytoskeleton in our cellular model of DS. In the trisomic model, the underlying conditions can trigger alterations in neurite

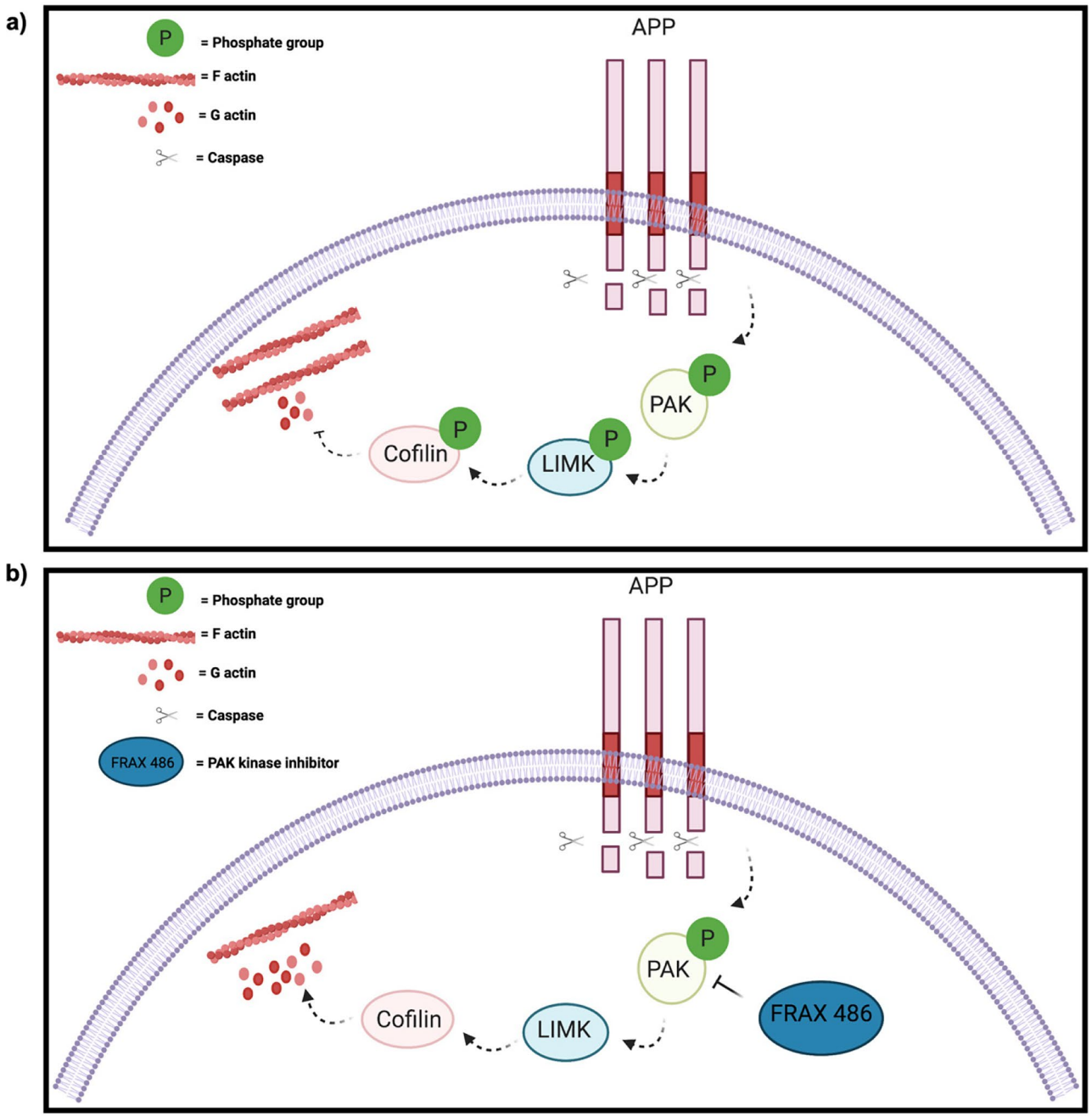

Fig. 5 Proposed model on the impact of APP overexpression and PAK pathway on actin cytoskeleton dynamics in the trisomic cell line. **a** CTb cells display conditions, such as APP overexpression, increased C-terminal cleavage of APP, increased caspase activity, and increased PAK1 phosphorylation. The latter results in excessive phosphorylation of LIMK and cofilin, and an increase of the filamentous form of actin that can impair neurite outgrowth. **b** Neurite growth alterations can be reversed after treatment with the PAK1 inhibitor, FRAX 486. The mechanism could be related to the modification of the LIMK-cofilin-actin pathway activity towards levels comparable to those of the euploid condition. Images were created with BioRender.com

outgrowth. Such conditions may be, but are not limited to, APP overexpression, increased APP C-terminal cleavage, increased caspase activity, and PAK1 hyperphosphorylation (Fig. 5a). The increase in the formation of processes in CTb cells, after incubation with FRAX 486, may result from a greater dynamic between monomeric and filamentous actin via PAK-LIMK-cofilin (Fig. 5b). In this last point, we refer to the fact that the addition of FRAX 486 to a cellular model of DS such as CTb cells promotes the formation of new neurites but, at the same time, appears to increase the loss of processes, possibly due to an increased dynamics of the actin cytoskeleton via the PAK pathway.

In addition, it should be considered that neurite outgrowth and axon guidance depend on growth cone structures such as lamellipodia and filopodia (composed mainly of microtubules and actin cytoskeleton) (Lewis and Brigdman 1992) and their dynamics, such as actin turnover in the leading edge (Goor et al. 2012). In fact, axon elongation has been observed to arrest after adding cytochalasin-b (a compound that depolymerizes F-actin) in the dorsal lumbosacral root ganglia of chick embryos (Yamada et al. 1970). Furthermore, disorganized extensions and lamellipodia protuberances surrounding the soma have been described in mouse neurons after transfection with specific PAK1-shRNA, further suggesting that the formation of polarized lamellipodia in neuronal migration depends on the localized kinase activity of PAK1 and that its main function is to promote organized neurite outgrowth (Causeret et al. 2009).

Thus, we suggest that the increased length, branching, and formation of new processes can be attributed to the fact that FRAX 486 could stimulate the dynamics of the actin cytoskeleton and influence neurite growth processes in CTb cells. Therefore, decreasing PAK1 phosphorylation on CTb cells could influence dynamic processes that include neurite elongation, such as lamellipodia and filopodia (Goldberg and Burmeister 1986).

Although in the trisomic model, PAK may be hyperphosphorylated for various reasons, including Down syndrome cell adhesion molecule (DSCAM) overexpression (Pérez-Núñez et al. 2016), it is important to highlight the benefit of inferring in a therapeutic target that more directly affects neurite outgrowth and remodeling and that appears as a common link between several DS-related overexpressed proteins, such as APP and DSCAM.

In this regard, PAK has been proposed as a therapeutic target in the past, as previous studies have related mutations in the PAK3 gene in non-syndromic X-linked mental retardation (MRX) (Allen et al. 1998). On the other hand, the inhibition of the catalytic activity of PAK partially improves some anomalies related to fragile X syndrome (FXS), such as synaptic morphology, synaptic plasticity, and behavior in the forebrain of fragile X mental retardation 1 (FMR1) mice knockout, an animal model of FXS (Hayashi et al. 2007b). Furthermore, FRAX 486 treatment rescues the spine density phenotype and behavioral abnormalities such as hyperactivity and repetitive movements in a mouse model of FXS (Dolan et al. 2013).

Taking the existing prior information and the concurring results described herein, we suggest PAK as a possible therapeutic target, since by antagonizing its function in a hyperphosphorylated state, it favors the increase of parameters related to a greater branching of cellular processes, such as the emission of new processes (OBI), the length of the processes, the crossings of the Sholl ring, and the loss of processes (DBI), in the cellular model of DS, CTb cells.

Conclusions

The overexpression of genes that occurs in the trisomic condition is directly or indirectly related to all the pathological characteristics that patients with DS present. Among them, the cognitive deficit is the most limiting condition for daily life. The changes that patients with DS may undergo at the cerebral level can be seen reflected in morphological alterations of the neuronal cells of the cerebral cortex and hippocampus among others. In our study, we observed that the addition of a PAK inhibitor, FRAX 486, to in vitro neuronal model of DS, CTb cells, increases the length of processes, Sholl ring crossings, the formation of new processes, and increases the loss of processes, suggesting that FRAX 486 may increase growth processes and remodeling. This study provides the basis for continuing to work with a FRAX 486 in animal models of DS, where behavioral studies can also be carried out, and suggests that PAK1 is a pharmacological target in Down syndrome.

Author Contribution N.B. carried out most experiments and wrote the main manuscript. R. P-N. assisted with blotting experiments and data analysis. B.G. conducted part of FRAX486 inhibition experiments. A. B. designed the algorithms for morphological analysis. C.A. assisted with blotting experiments and morphological analysis. K.P. and V.J. assisted with blotting experiments related to APP Δ665 detection and caspase activity. J-V. B. assisted in PAK1 phosphorylation and activity experiments. A.M. C assisted in planning, data analysis, and manuscript text. P.C. assisted in all aforementioned aspects of the research and writing of the text. All authors reviewed the manuscript and are aware it is being submitted to this journal in its present version.

Funding This work was funded by FONDECYT Grant #1130241, 1161450 (Chile) to PC, the Fondation pour la Recherche sur le Cerveau (FRC) and the Fondation Jérôme Lejeune (J-V. B., France), CONICYT for funding of Basal Centre, CeBiB, FB0001 and P09-022-F from ICM-ECONOMIA (Chile), and CONICYT grant #21120728 (Chile).

Availability of Data and Materials Upon request.

Declarations

Ethical Approval N/A.

Competing Interests PC holds patent protection for the CNh and CTb cell lines.

References

Allen KM, Gleeson JG, Bagrodia S, Partington MW, MacMillan JC, Cerione RA, Mulley JC, Walsh CA (1998) PAK3 mutation in nonsyndromic X-linked mental retardation. Nat Genet 20(1):25–30. https://doi.org/10.1038/1675

Antonarakis SE (1993) Human chromosome 21: genome mapping and exploration, circa 1993. Trends Genet 9(4):142–148. https://doi.org/10.1016/0168-9525(93)90210-9

Binley KE, Ng WS, Tribble JR, Song B, Morgan JE (2014) Sholl analysis: a quantitative comparison of semi-automated methods. J Neurosci Methods 225:65–70. https://doi.org/10.1016/j.jneumeth.2014.01.017

Bokoch GM (2003) Biology of the p21-activated kinases. Annu Rev Biochem 72:743–781. https://doi.org/10.1146/annurev.biochem.72.121801.161742

Cárdenas AM, Rodríguez MP, Cortés MP, Alvarez RM, Wei W, Rapaport SI, Shimahara T, Caviedes R, Caviedes P (1999) Calcium signals in cell lines derived from the cerebral cortex of normal and trisomy 16 mice. NeuroReport 10(2):363–369. https://doi.org/10.1097/00001756-199902050-00028

Causeret F, Terao M, Jacobs T, Nishimura YV, Yanagawa Y, Obata K, Hoshino M, Nikolic M (2009) The p21-activated kinase is required for neuronal migration in the cerebral cortex. Cereb Cortex 19(4):861–875. https://doi.org/10.1093/cercor/bhn133

Cullum L, Liebman J (1969) The association of congenital heart disease with down's syndrome (mongolism). Am J Cardiol 24(3):354–357. https://doi.org/10.1016/0002-9149(69)90428-7

De toma I, Ortega M, Aloy P, Sabidó E, Dierssen M. (2019) DYRK1A overexpression alters cognition and neural-related proteomic pathways in the hippocampus that are rescued by Green tea extract and/or environmental enrichment. Front Mol Neurosci 12:272. https://doi.org/10.3389/fnmol.2019.00272

De Toma I, Ortega M, Catuara-Solarz S, Sierra C, Sabidó E, Dierssen M (2020) Re-establishment of the epigenetic state and rescue of kinome deregulation in Ts65Dn mice upon treatment with green tea extract and environmental enrichment. Sci Rep 10(1):16023. https://doi.org/10.1038/s41598-020-72625-z

Dierssen M, Benavides-Piccione R, Martínez-Cué C, Estivill X, Flórez J, Elston GN, DeFelipe J (2003) Alterations of neocortical pyramidal cell phenotype in the Ts65Dn mouse model of down syndrome: Effects of environmental enrichment. Cereb Cortex 13(7):758–764. https://doi.org/10.1093/cercor/13.7.758

Dolan BM, Duron SG, Campbell DA, Vollrath B, Rao BSS, Ko HY, Lin GG, Govindarajan A, Choi SY, Tonegawa S (2013) Rescue of fragile X syndrome phenotypes in Fmr1 KO mice by the small-molecule PAK inhibitor FRAX486. Proc Natl Acad Sci USA 110(14):5671–5676. https://doi.org/10.1073/pnas.1219383110

Doran E, Keator D, Head E, Phelan MJ, Kim R, Totoiu M, Barrio JR, Small GW, Potkin SG, Lott IT (2017) Down syndrome, partial trisomy 21, and absence of Alzheimer's disease: the role of APP. J Alzheimers Dis 56(2):459–470. https://doi.org/10.3233/jad-160836

Dubos A, Combeau G, Bernardinelli Y, Barnier JV, Hartley O, Gaertner H, Boda B, Muller D (2012) Alteration of synaptic network dynamics by the intellectual disability protein PAK3. J Neurosci 32(2):519–527. https://doi.org/10.1523/JNEUROSCI.3252-11.2012

Edwards DC, Sanders LC, Bokoch GM, Gill GN (1999) Activation of LIM-kinase by Pak1 couples Rac/Cdc42 GTPase signalling to actin cytoskeletal dynamics. Nat Cell Biol 1(5):253–259. https://doi.org/10.1038/12963

Fong CT, Brodeur GM (1987) Down's syndrome and leukemia: epidemiology, genetics, cytogenetics and mechanisms of leukemogenesis. Review Cancer Genet Cytogenet 28(1):55–76. https://doi.org/10.1016/0165-4608(87)90354-2

García-Segura LM, Pérez-Márquez J (2014) A new mathematical function to evaluate neuronal morphology using the Sholl analysis. J Neurosci Methods 226:103–109. https://doi.org/10.1016/j.jneumeth.2014.01.016

Goldberg DJ, Burmeister DW (1986) Stages in axon formation: observations of growth of Aplysia axons in culture using video-enhanced contrast-differential interference contrast microscopy. J Cell Biol 103(5):1921–1931. https://doi.org/10.1083/jcb.103.5.1921

Goor DV, Hyland C, Schaefer AW, Forscher P (2012) The role of actin turnover in retrograde actin network flow in neuronal growth cones. PloS ONE 7(2):e30959. https://doi.org/10.1371/journal.pone.0030959

Graaf GD, Buckley F, Skotko B (2020) Estimation of the number of people with Down syndrome in Europe. Eur J Human Genet 29(3):402–410. https://doi.org/10.1038/s41431-020-00748-y

Harms FL, Kloth K, Bley A, Denecke J, Santer R, Lessel D, Hempel M, Kutsche K (2018) Activating mutations in PAK1, encoding p21-activated kinase 1, cause a neurodevelopmental disorder. Am J Hum Genet 103(4):579–591. https://doi.org/10.1016/j.ajhg.2018.09.005

Hassold T, Hunt P (2001) To err (meiotically) is human: the genesis of human aneuploidy. Nat Rev Genet 2(4):280–291. https://doi.org/10.1038/35066065

Hattori M, Fujiyama A, Taylor TD, Watanabe H, Yada T, Park HS, Toyoda A, Ishii K, Totoki Y, Choi DK, Soeda E, Ohki M, Takagi T, Sakaki Y, Taudien S, Blechschmidt K, Polley A, Menzel U, Delabar J, Kumpf K, Lehmann R, Patterson D, Reichwald K, Rump A, Schillhabel M, Schudy A, Zimmermann W, Rosenthal A, Kudoh J, Shibuya K, Kawasaki K, Asakawa S, Shintani A, Sasaki T, Nagamine K, Mitsuyama S, Antonarakis SE, Minoshima S, Shimizu N, Nordsiek G, Hornischer K, Brandt P, Scharfe M, Schön O, Desario A, Reichelt J, Kauer G, Blöcker H, Ramser J, Beck A, Klages S, Hening S, Riesselmann L, Dagand E, Haaf T, Wehrmeyer S, Borzym K, Gardiner K, Nizetic D, Francis F, Lehrach H, Reinhardt R, Yaspo ML (2000) The DNA sequence of human chromosome 21. Nature 405(6784):311–319. https://doi.org/10.1038/35012518

Hayashi K, Ohshima T, Hashimoto M, Mikoshiba K (2007a) Pak1 regulates dendritic branching and spine formation. Dev Neurobiol 67(5):655–669. https://doi.org/10.1002/dneu.20363

Hayashi ML, Rao BSS, Seo JS, Choi HS, Dolan BM, Choi SY, Chattarji S, Tonegawa S (2007b) Inhibition of p21-activated kinase rescues symptoms of fragile X syndrome in mice. Proc Natl Acad Sci U S A 104(27):11489–11494. https://doi.org/10.1073/pnas.0705003104

Huang W, Zhou Z, Asrar S, Henkelman M, Xie W, Jia Z (2011) p21-activated kinases 1 and 3 control brain size through coordinating neuronal complexity and synaptic properties. Mol Cell Biol 31(3):388–403. https://doi.org/10.1128/MCB.00969-10

Huo HQ, Qu ZY, Yuan F, Ma L, Yao L, Xu M, Hu Y, Ji J, Bhattacharyya A, Zhang SC, Liu Y (2018) Modeling Down syndrome with patient iPSCs reveals cellular and migration deficits of GABAergic neurons. Stem Cell Reports 10(4):1251–1266. https://doi.org/10.1016/j.stemcr.2018.02.001

Jain S, Watts CA, Chung WCJ, Welshhans K (2020) Neurodevelopmental wiring deficits in the Ts65Dn mouse model of Down syndrome. Neurosci Lett 714:134569. https://doi.org/10.1016/j.neulet.2019.134569

Kang J, Lemaire HG, Unterbeck A, Salbaum JM, Masters CL, Grzeschik KH, Multhaup G, Beyreuther K, Müller-Hill B (1987) The precursor of Alzheimer's disease amyloid A4 protein resembles a cell-surface receptor. Nature 325(6106):733–736. https://doi.org/10.1038/325733a0

Korenberg JR, Pulst SM, Neve RL, West R (1989) The Alzheimer amyloid precursor protein maps to human chromosome 21 bands q21.105-q21.05. Genomics 5(1):124–7. https://doi.org/10.1016/0888-7543(89)90095-5

Kreis P, Barnier JV (2009) PAK signalling in neuronal physiology. Cell Signal 21(3):384–393. https://doi.org/10.1016/j.cellsig.2008.11.001

Kreis P, Thévenot E, Rousseau V, Boda B, Muller D, Barnier JV (2007) The p21-activated kinase 3 implicated in mental retardation regulates spine morphogenesis through a Cdc42-dependent pathway. J Biol Chem 282(29):21497–21506. https://doi.org/10.1074/jbc.M703298200

Krivit W, Good RA (1957) Simultaneous occurrence of mongolism and leukemia; report of a nationwide survey. AMA J Dis Child 94(3):289–293. https://doi.org/10.1001/archpedi.1957.04030040075012

Lewis AK, Bridgman PC (1992) Nerve growth cone lamellipodia contain two populations of actin filaments that differ in organization and polarity. J Cell Biol 119(5):1219–1243. https://doi.org/10.1083/jcb.119.5.1219

Licciulli S, Maksimoska J, Zhou C, Troutman S, Kota S, Liu Q, Duron S, Campbell D, Chernoff J, Field J, Marmorstein R, Kissil JL (2013) FRAX 597, a small molecule inhibitor of the p21-activated kinases, inhibits tumorigenesis of neurofibromatosis type 2 (NF2)-associated Schwannomas. J Biol Chem 288(40):29105–29114. https://doi.org/10.1074/jbc.M113.510933

López-Cabrera JD, Hernández-Pérez LA, Orozco-Morales R, Lorenzo-Ginori JV (2020) New morphological features based on the Sholl analysis for automatic classification of traced neurons. J Neurosci Methods 343:108835. https://doi.org/10.1016/j.jneumeth.2020.108835

Lu DC, Rabizadeh S, Chandra S, Shayya RF, Ellerby LM, Ye X, Salvesen GS, Koo EH, Bredesen DE (2000) A second cytotoxic proteolytic peptide derived from amyloid beta-protein precursor. Nat Med 6(4):397–404. https://doi.org/10.1038/74656

Mai CT, Isenburg JL, Canfield MA, Meyer RE, Correa A, Alverson CJ, Lupo PJ, Riehle-Colarusso T, Cho SJ, Aggarwal D, Kirby RS, Network NBDP (2019) National population – based estimates for major birth defects, 2010–2014. Birth Defects Res 111(18):1420–1435. https://doi.org/10.1002/bdr2.1589

Manfredi-Lozano M, Leysen V, Adamo M, Paiva I, Rovera R, Pignat JM, Timzoura FE, Candlish M, Eddarkaoui S, Malone SA, Silva MSB, Trova S, Imbernon M, Decoster L, Cotellessa L, Tena-Sempere M, Claret M, Paoloni-Giacobino A, Plassard D, Paccou E, Vionnet N, Acierno J, Maceski AM, Lutti A, Pfrieger F, Rasika S, Santoni F, Boehm U, Ciofi P, Buée L, Haddjeri N, Boutillier AL, Kuhle J, Messina A, Draganski B, Giacobini P, Pitteloud N, Prevot V (2022) GnRH replacement rescues cognition in Down syndrome. Science 377(6610):eabq4515. https://doi.org/10.1126/science.abq4515

Manser E, Leung T, Salihuddin H, Zhao ZS, Lim L (1994) A brain serine/threonine protein kinase activated by Cdc42 and Rac1. Nature 367(6458):40–46. https://doi.org/10.1038/367040a0

Manser E, Huang HY, Loo TH, Chen XQ, Dong JM, Leung T, Lim L (1997) Expression of constitutively active alpha-PAK reveals effects of the kinase on actin and focal complexes. Mol Cell Biol 17(3):1129–1143. https://doi.org/10.1128/MCB.17.3.1129

Marin-Padilla M (1976) Pyramidal cell abnormalities in the motor cortex of a child with Down's syndrome. A Golgi study. J Comp Neurol 167(1):63–81. https://doi.org/10.1002/(ISSN)1096-9861, https://doi.org/10.1002/cne.v167:1, https://doi.org/10.1002/cne.901670105

Martin GA, Bollag G, McCormick F, Abo A (1995) A novel serine kinase activated by rac1/CDC42Hs-dependent autophosphorylation is related to PAK65 and STE20. EMBO J 14(9):1970–1978. https://doi.org/10.1002/j.1460-2075.1995.tb07189.x

Masters CL, Simms G, Weinman NA, Multhaup G, McDonald BL, Beyreuther K (1985) Amyloid plaque core protein in Alzheimer disease and Down syndrome. Proc Natl Acad Sci U S A 82(12):4245–4249. https://doi.org/10.1073/pnas.82.12.4245

McCarron M, McCallion P, Reilly E, Dunne P, Carroll R, Mulryan N (2017) A prospective 20-year longitudinal follow-up of dementia in persons with Down syndrome. J Intellect Disabil Res 61(9):843–852. https://doi.org/10.1111/jir.12390

McPhie DL, Coopersmith R, Hines-Peralta A, Chen Y, Ivins KJ, Manly SP, Kozlowski MR, Neve KA, Neve RL (2003) DNA synthesis and neuronal apoptosis caused by familial Alzheimer disease mutants of the amyloid precursor protein are mediated by the p21 activated kinase PAK3. J Neurosci 23(17):6914–6927. https://doi.org/10.1523/JNEUROSCI.23-17-06914.2003

Nguyen TVV, Galvan V, Huang W, Banwait S, H, Zhang J, Bredesen DE. (2008) Signal transduction in Alzheimer disease: p21-activated kinase signaling requires C-terminal cleavage of APP at Asp664. J Neurochem 104(4):1065–1080. https://doi.org/10.1111/j.1471-4159.2007.05031.x

Opazo P, Saud K, Saint Pierre M, Cárdenas AM, Allen DD, Segura-Aguilar J, Caviedes R, Caviedes P (2006) Knockdown of amyloid precursor protein normalizes cholinergic function in a cell line derived from the cerebral cortex of a trisomy 16 mouse: an animal model of down syndrome. J Neurosci Res 84(6):1303–1310. https://doi.org/10.1002/jnr.21035

Oster-Granite ML (1986) The neurobiologic consequences of autosomal trisomy in mice and men. Brain Res Bull 16(6):767–771. https://doi.org/10.1016/0361-9230(86)90073-0

Pérez-Núñez R, Barraza N, Gonzalez-Jamett A, Cárdenas AM, Barnier JV, Caviedes P (2016) Overexpressed Down syndrome cell adhesion molecule (DSCAM) deregulates p21-activated kinase (PAK) activity in an in vitro neuronal model of Down syndrome: consequences on cell process formation and extension. Neurotox Res 30(1):76–87. https://doi.org/10.1007/s12640-016-9613-9

Pinter JD, Eliez S, Schmitt JE, Capone GT, Reiss AL (2001) Neuroanatomy of Down's syndrome: a high-resolution MRI study. AM J Psychiatry 158(10):1659–1665. https://doi.org/10.1176/appi.ajp.158.10.1659

Prasher VP, Farrer MJ, Kessling AM, Fisher EM, West RJ, Barber PC, Butler AC (1998) Molecular mapping of Alzheimer-type dementia in Down's syndrome. Ann Neurol 43(3):380–383. https://doi.org/10.1002/ana.410430316

Pritchard MA, Kola I (1999) The "gene dosage effect" hypothesis versus the "amplified developmental instability" hypothesis in Down syndrome. J Neural Transm Suppl 57:293–303. PMID: 10666684

Rashid T, Banerjee M, Nikolic M (2001) Phosphorylation of Pak1 by the p35/Cdk5 kinase affects neuronal morphology. J Biol Chem 276(52):49043–49052. https://doi.org/10.1074/jbc.M105599200

Raz N, Torres IJ, Briggs SD, Spencer WD, Thornton AE, Loken WJ, Gunning FM, McQuain JD, Driesen NR, Acker JD (1995) Selective neuroanatomic abnormalities in Down's syndrome and their cognitive correlates: evidence from MRI morphometry. Neurology 45(2):356–366. https://doi.org/10.1212/WNL.45.2.356

Rojas G, Cárdenas AM, Fernández-Olivares P, Shimahara T, Segura-Aguilar J, Caviedes R, Caviedes P (2008) Effect of the knockdown of amyloid precursor protein on intracellular calcium increases in a neuronal cell line derived from the cerebral cortex of a trisomy 16 mouse. Exp Neurol 209(1):234–242. https://doi.org/10.1016/j.expneurol.2007.09.024

Rousseau V, Goupille O, Morin N, Barnier JV (2003) A new constitutively active brain PAK3 isoform displays modified specificities

toward Rac and Cdc42 GTPases. J Biol Chem 278(6):3912–3920. https://doi.org/10.1074/jbc.M207251200

Strydom A, Coppus A, Blesa R, Danek A, Fortea J, Hardy J, Levin J, Nuebling G, Rebillat AS, Ritchie C, Duijn CV, Zaman S, Zetterberg H (2018) Alzheimer's disease in Down syndrome: an overlooked population for prevention trials. Alzheimers Dement (NY) 4:703–713. https://doi.org/10.1016/j.trci.2018.10.006

Takashima S, Becker LE, Armstrong DL, Chan FW (1981) Abnormal neuronal development in the visual cortex of the human fetus and infant with down's syndrome. A quantitative and qualitative golgi study. Brain Res 225(1):1–21. https://doi.org/10.1016/0006-8993(81)90314-0

Tang XY, Xu L, Wang J, Hong Y, Wang Y, Zhu Q, Wang D, Zhang XY, Liu CY, Fang KH, Han X, Wang S, Wang X, Xu M, Bhattacharyya A, Guo X, Lin M, Liu Y (2021) DSCAM/PAK1 pathway suppression reverses neurogenesis deficits in iPSC-derived cerebral organoids from patients with Down syndrome. J Clin Invest 131(12):e135763. https://doi.org/10.1172/JCI135763.

Weidemann A, Paliga K, Dürrwang U, Reinhard FB, Schuckert O, Evin G, Masters CL (1999) Proteolytic processing of the alzheimer's disease amyloid precursor protein within its cytoplasmic domain by caspase-like proteases. J Biol Chem 274(9):5823–5829. https://doi.org/10.1074/jbc.274.9.5823

Wisniewski KE (1990) Down syndrome children often have brain with maturation delay, retardation of growth, and cortical dysgenesis. Am J Med Genet Suppl 7:274–281. https://doi.org/10.1002/ajmg.1320370755

Whooten R, Schmitt J, Schwartz A (2018) Endocrine manifestations of Down syndrome. Curr Opin Endocrinol Diabetes Obes 25(1):61–66. https://doi.org/10.1097/MED.0000000000000382

Yamada KM, Spooner BS, Wessells NK (1970) Axon growth: roles of microfilaments and microtubules. Proc Natl Acad Sci USA 66(4):1206–1212. https://doi.org/10.1073/pnas.66.4.1206

Zhao ZS, Manser E, Chen XQ, Chong C, Leung T, Lim L (1998) A conserved negative regulatory region in αPAK: Inhibition of PAK kinases reveals their morphological roles downstream of Cdc42 and Rac1 ABSTRACT. Mol Cell Biol 18(4):2153–2163. https://doi.org/10.1128/MCB.18.4.2153